

Quantum ferroelectric instabilities in superconducting SrTiO₃

J. R. Arce-Gamboa¹, G. G. Guzmán-Verri^{1,2*}

¹*Centro de Investigación en Ciencia e Ingeniería de Materiales (CICIMA),
Universidad de Costa Rica, San José, Costa Rica 11501 and*

²*Materials Science Division, Argonne National Laboratory, Argonne, Illinois, USA 60439,*

(Dated: November 1, 2018)

We examine the effects of strain and cation substitution on the superconducting phase of polar semiconductors near a ferroelectric quantum phase transition with a model that combines a strong coupling theory of superconductors with a standard microscopic framework for displacive polar modes coupled to strain degrees of freedom. Our calculations reveal that the superconducting transition temperature T_c is enhanced by proximity to the ferroelectric instability from the disordered side, while it is generally suppressed in the ordered phase due to its increase in dielectric stiffness and a reduction of critical fluctuations from dipolar induced anisotropies. The condensation of the pairing phonon excitations generates a kink in T_c at a charge density that is generally lower than that of the quantum critical point (QCP) and where both superconducting and ferroelectric orders set in. We apply our model to SrTiO₃ and find that the antiadiabatic limit places the kink nearly at its QCP. As the QCP is pushed to higher charge densities with either tuning parameter, we find that the dome narrows and sharpens. Our model is in qualitative and fair quantitative agreement with the recent observation of overlapping ferroelectric-like and superconducting instabilities in n-doped Sr_{1-x}Ca_xTiO₃ and strain tuning of T_c in n-doped SrTiO₃. We compare our results to previous models invoking order-disorder lattice dynamics to describe the pairing excitations.

I. INTRODUCTION

Strontium titanate (STO) is the first superconducting (SC) oxide to be discovered more than half a century ago¹. Upon doping, it exhibits dome-shaped superconductivity²⁻⁵ similar to the well-known cuprates at unusually low charge carrier concentrations ($< 10^{18} \text{ cm}^{-3}$)⁶⁻⁹, dubbing STO as the most dilute superconductor¹⁰. Since its observation, the origin of the pairing mechanism between its charge carriers has posed a long-standing problem in condensed matter physics, as the conventional Bardeen-Cooper-Schrieffer theory of superconductors requires the so-called adiabatic limit of electron-phonon coupling in which the characteristic energy scale of the charge carriers (the Fermi temperature T_F) is much larger than that of the phonons (the Debye temperature T_D)¹¹. STO is unusual in that it is outside this limit as $T_F \simeq 13 \text{ K}$ ¹⁰ and $T_D \simeq 400 \text{ K}$ ¹². Though several models have been put forward¹³⁻¹⁶, and experiments have constrained possible pairing mechanisms between its charge carriers¹⁷, there is still no consensus on a theory of superconductivity in dilute polar semiconductors such as doped STO¹⁸.

Somewhat recently, Rowley *et al.*¹⁹ have suggested a connection between quantum criticality and superconductivity in STO, and Edge *et al.*²⁰ have put forward a concrete model. Within this framework, a QCP that separates competing ferroelectric (FE) and paraelectric (PE) ground states generates highly collective low energy phonon excitations which induce an instability in the metallic phase and pair the charge carriers to form Cooper pairs. A dome arises because the quantum FE fluctuations pair up the charge carriers at low doping levels, though there are not enough of

them to provide a robust superconductivity. As the density increases, so does T_c until the fluctuations become ineffective at pairing due to screening by the carriers themselves. Though STO is not within the adiabatic limit, the model provides a good description of its SC dome, and it has received recent experimental support²¹⁻²³.

In conventional FEs, the relevant low energy lattice excitations are zone-center transverse optic (TO) phonons which break spatial inversion symmetry and trigger a phase with a spontaneous, reversible polarization upon condensation. In pure STO, such a transition is aborted by quantum fluctuations of the polarization order parameter²⁴ and, instead, incipient FE behavior is observed in which the dielectric constant grows enormously ($\simeq 10^4$) and the phonon frequencies soften down to lowest observed temperatures without condensing²⁵. Long-range FE order has been induced by tensile stress²⁶, oxygen isotope exchange²⁷, or cation substitution²⁸. At the QCP, the phonon excitations become gapless, and at finite temperatures above it but well below T_D ²⁹, quantum criticality sets in generating unusual behavior, such as a T^{-2} dependence in the dielectric susceptibility distinct from that of the neighboring PE and FE phases¹⁹.

To model the pairing excitations between carriers, one-dimensional transverse Ising models with short-range interactions have been invoked and solved within a mean field approximation^{20,30,31}. However, the soft collective vibrational excitations described by such models are not normal modes of the lattice but rather unstable pseudospin waves with relaxational dynamics, which are typical of order-disorder (OD) FEs such as potassium dihydrogen phosphate (KH₂PO₄)³². STO, on the other hand, is a perovskite with a low temperature tetragonal

PE phase which exhibits displacive behavior with a resonant soft TO mode that fully accounts for the dielectric constant and remains undamped down to the lowest observed temperatures^{19,25,33}, even when the lattice instability is approached by oxygen isotope substitution where it has been suggested that the effects of an OD component may become important^{34,35}. Moreover, FE transitions in perovskites are generally understood as resulting from the competition between a PE state favored by short-range repulsive forces and a FE phase favored by long-ranged and anisotropic dipole interactions that arise from their mixed covalent-ionic bonding character.³⁶ The aim of this paper is to describe the SC phase that emerges from a pairing excitation that corresponds to a displacive soft TO phonon.

We use a self-consistent phonon approximation (SCPA) to study the quantum statistical mechanics of our model Hamiltonian which includes local thermal and quantum fluctuations of the order parameter. This allows us to self-consistently calculate the doping and strain dependence of T_c , as well the FE transition temperature T_{fe} , phonon energies and polarization order parameter. We neglect the effects of band narrowing due to polaron formation, which could have strong effects on the correlations³⁷.

We find that proximity to the QCP favors superconductivity from the PE side, but T_c decreases on the ordered side due to a reduction of the critical fluctuations from dipolar induced anisotropies and the dielectric stiffening by the spontaneous polarization. This generates a kink in the SC dome at a characteristic charge density that is generally lower than that of the QCP and where the SC and FE orders set in. As the QCP is pushed to higher charge densities with cation substitution or tensile strain so the FE phase increasingly overlaps with the SC phase, the dome narrows and sharpens. Though we do not make any *a-priori* assumptions that the pairing fluctuations are quantum critical, we find that the antiadiabatic limit places the kink nearly at the QCP and within the QC region. While our results are in qualitative agreement with the essentials of the OD models, there are significant qualitative differences. Though our model produces a dome which is narrower than the observed one, its phase diagram is in overall agreement with recent experiments in n-doped $\text{Sr}_{1-x}\text{Ca}_x\text{TiO}_3$ (STO:Ca-x)²¹ and the observed strain tuning of T_c in n-doped STO^{23,38,39}

II. MODEL

Following Ref. [20], our starting point is the McMillian formula⁴⁰ for the SC coupling constant,

$$\lambda(n, T, P) = \int_0^\infty \alpha_{e-ph}^2(\omega) F(\omega) \frac{d\omega}{\omega},$$

where $\alpha_{e-ph}(\omega)$ is the electron-phonon coupling, $F(\omega) = \sum_{\mathbf{q}, \mu} \delta(\omega - \Omega_{\mathbf{q}\mu})$, is the spectral density at frequency ω , and $\Omega_{\mathbf{q}\mu}$ ($\mu = 1, 2, 3$) is the phonon energy at wave vector \mathbf{q} . Generally, it is not expected that charge carriers couple to long-wavelength TO phonons.⁴¹ For perovskite lattices such as that of STO, this is indeed the case but only when \mathbf{q} is along a principal axis. Away from such special directions, coupling occurs due to cubic anisotropy.⁴² While such finite coupling still depends on $\Omega_{\mathbf{q}\mu}$, we make the simplifying assumption that α_{e-ph} is independent of it. Thus,

$$\lambda(n, T, P) = \alpha_{e-ph}^2 \sum_{\mathbf{q}, \mu} \frac{1}{\Omega_{\mathbf{q}\mu}}, \quad (1)$$

where the sum over \mathbf{q} runs over the entire Brillouin zone. We note that despite this assumption λ does not diverge: The largest contributions occur at the FE transition where the TO phonons become gapless and have a dispersion $\Omega_{\mathbf{q}} \propto q$ [see Eq.(5b) below]. By taking the continuum limit of Eq. (1) over a sphere of wave vector cutoff radius Λ , we find that $\lambda \propto \int d^3\mathbf{q}/\Omega_{\mathbf{q}} \propto \int_0^\Lambda dq q^2/q \propto \Lambda^2$.

T_c is calculated from the strong-coupling theory,²⁰

$$1 = \frac{\lambda(n, T_c, P)}{2\pi^2} \int_{-\epsilon_F}^0 d\epsilon N(\epsilon) \frac{\tanh(\beta_c \epsilon/2)}{\epsilon}, \quad (2)$$

where $N(\epsilon) \simeq \sqrt{\epsilon + \epsilon_F}$ is the electron density of states near the Fermi level ϵ_F , and $\beta_c = (k_B T_c)^{-1}$.

We now need a model for the phonon excitations. We consider a standard model Hamiltonian for displacive FEs with normal mode coordinates that describe local displacements $\mathbf{Q}_i = (Q_{ix}, Q_{iy}, Q_{iz})$ in the unit cell i that are associated with the soft TO mode, the condensation of which is driven by the dipolar force and leads to the FE transition³². We also consider elastic strains η_α coupled to the displacements \mathbf{Q}_i . We write the components of the strain tensor in the usual Voigt notation: $\eta_1 \equiv \epsilon_{xx}$, $\eta_2 \equiv \epsilon_{yy}$, $\eta_3 \equiv \epsilon_{zz}$, $\eta_4 = 2\epsilon_{yz}$, $\eta_5 = 2\epsilon_{xz}$, and $\eta_6 = 2\epsilon_{xy}$.

The Hamiltonian is as follows⁴³,

$$H = H_Q + H_\eta + H_{Q\eta}, \quad (3)$$

where,

$$H_Q = \frac{1}{2} \sum_i |\Pi_i|^2 + \frac{\kappa}{2} \sum_i |\mathbf{Q}_i|^2 + \frac{\alpha}{4} \sum_i |\mathbf{Q}_i|^4 + \frac{\gamma}{2} \sum_{i, \nu \neq \nu'} Q_{i\nu}^2 Q_{i\nu'}^2 - \frac{1}{2} \sum_{ij\nu\nu'} v_{ij}^{\nu\nu'} Q_{i\nu} Q_{j\nu'}, \quad (4a)$$

$$H_\eta = \frac{1}{2} \sum_{i, \mu=1}^6 C_{\mu\mu'} \eta_{\mu i} \eta_{\mu' i} + P \sum_{i, \mu=1}^3 \eta_{\mu i}, \quad (4b)$$

$$\begin{aligned}
H_{Q\eta} = & -e_a \sum_i (\eta_{1i} + \eta_{2i} + \eta_{3i}) |\mathbf{Q}_i|^2 \\
& - e_t \sum_i [\eta_{1i} (2Q_{ix}^2 - Q_{iy}^2 - Q_{iz}^2) \\
& \quad + \eta_{2i} (2Q_{iy}^2 - Q_{ix}^2 - Q_{iz}^2) \\
& \quad + \eta_{3i} (2Q_{iz}^2 - Q_{ix}^2 - Q_{iy}^2)] \\
& - e_r \sum_i (Q_{ix}Q_{iy}\eta_{6i} + Q_{ix}Q_{iz}\eta_{5i} + Q_{iy}Q_{iz}\eta_{4i}).
\end{aligned} \tag{4c}$$

Here, $\mathbf{\Pi}_i$ is the conjugate momentum of \mathbf{Q}_i , and $v_{ij}^{\nu\nu'}$ ($\nu, \nu' = x, y, z$) is the dipolar interaction tensor with Fourier transform $v_{\mathbf{q}}^{\nu\nu'} = [\frac{1}{3}C^2 - B^2q^2] \delta_{\nu\nu'} - C^2 \frac{q_\nu q_{\nu'}}{q^2}$, where $q = |\mathbf{q}|$ and B and C are constants that depend on the lattice structure⁴⁴. κ is the lattice stiffness; α and γ are coefficients of the isotropic and anisotropic cubic anharmonicities, respectively. e_a, e_t , and e_r are coupling constants between the polar and strain degrees of freedom; $C_{\mu\mu'}$ ($\mu, \mu' = 1, 2, \dots, 6$) is the elastic constant tensor in the cubic phase, and P is a hydrostatic pressure, both in units of energy (the usual elastic constants and homogeneous stresses are given by $C_{\mu\mu'}a^{-3}$ and Pa^{-3} where $a \simeq 3.9 \text{ \AA}$ is the lattice constant of the cubic structure). We consider fictitious negative hydrostatic pressures as a simple way to model the effects of tensile strain on the superconducting dome. Tensile strains are of course the experimentally relevant cases²⁶. We study the quantum statistical mechanics of the Hamiltonian (3) within SCPA⁴³. We consider the PE and FE phases separately.

A. PE phase

For simplicity, we will assume that the PE phase is cubic. Above T_{fe} , there is therefore a doubly degenerate TO phonon $\Omega_{\mathbf{q}}^{\perp}$ and a singlet longitudinal optic (LO) mode $\Omega_{\mathbf{q}}^{\parallel}$ with isotropic dispersions⁴⁵,

$$\left(\Omega_{\mathbf{q}}^{\parallel}\right)^2 = \left(\Omega_{\mathbf{q}}^{\perp}\right)^2 + C^2, \tag{5a}$$

$$\left(\Omega_{\mathbf{q}}^{\perp}\right)^2 = \left(\Omega_0^{\perp}\right)^2 + B^2q^2, \tag{5b}$$

where Ω_0^{\perp} is the TO mode at the zone center. As expected⁴⁶, the effect of the dipole force is to lift the triply degenerate mode of the cubic phase by gapping out the LO phonons.

Within SCPA, Ω_0^{\perp} is given as follows⁴³,

$$\left(\Omega_0^{\perp}\right)^2 = \omega_0^2 + (5\alpha + 2\gamma)\psi_0 - 2e_a\eta_a, \tag{6}$$

where $\omega_0 \equiv \sqrt{\kappa - v_0}$, is the frequency of a purely harmonic model and $v_0 \equiv C^2/3$ is the largest Fourier component of the dipole interaction; $\psi_0 = (2\omega)^{-1} \coth(\beta\omega/2)$ are local fluctuations of polarization with $\omega = \sqrt{\left(\Omega_0^{\perp}\right)^2 + v_0}$ and $\eta_a = \langle \eta_1 + \eta_2 + \eta_3 \rangle =$

$(e_a/C_a)(3\psi_0) - P/C_a$ is the volume strain. $\langle \dots \rangle$ denotes thermal average.

According to Eqs. (1) and (5), we therefore have,

$$\lambda(n, T_c, P) = \alpha_{e-ph}^2 \sum_{\mathbf{q}} \left(\frac{2}{\Omega_{\mathbf{q}}^{\perp}} + \frac{1}{\Omega_{\mathbf{q}}^{\parallel}} \right). \tag{7}$$

Note that the largest contributions to λ come from the critical mode $\Omega_{\mathbf{q}}^{\perp}$, as $\Omega_{\mathbf{q}}^{\parallel}$ is gapped out by the large depolarizing field.

We now parametrize the model parameters in order to describe the effects of doping and cation substitution on the phonon excitations. In the OD models^{20,30,31}, the quantum tunneling energy Γ between FE ground states with opposite polarization is chosen for such parametrization, as the effects of quantum fluctuations become important when Γ is comparable to the well-depth between such states. For displacive models, however, quantum fluctuations must be comparable to the structural differences between competing PE and FE ground states and generate zero-point energies comparable to the classical energy reduction⁴⁷. We therefore choose to parametrize such energy barrier, which in our model is proportional to $-\omega_0^4/\alpha$ at 0K. For simplicity, we keep α fixed and assume that all changes occur in ω_0 as follows,

$$\omega_0^2 \rightarrow \omega_0^2 \left[1 - b_2 \left(e^{\epsilon_F/b_1} - 1 \right) - g(x_r - x) \right], \tag{8}$$

where b_1, b_2, g are model parameters that will be fitted to experiments. $x_r = 0.018$ is the Ca concentration above which STO:Ca- x enters a glassy phase which we do not aim to describe here²⁸. This parametrization is constructed based on (i) the observation that doping destabilizes the FE phase^{20,21} while cation substitution stabilizes it; and (ii) the restriction that our model should generate simultaneous physically reasonable values for T_c and T_{fe} as well as $\Omega_{\mathbf{q}}$ in the relevant doping range. We will show below that Eq. (8) accomplishes this at the expense of narrowing the SC dome compared to the observed one. We have attempted to use the polynomial parametrization of the OD models, and while we can find a set of model parameters that fit the observed SC dome, we could not obtain physical values for T_{fe} and $\Omega_{\mathbf{q}}$. Clearly, this highlights the need for a theory to model these effects⁴².

Equations (2) and (5)-(8) are a self-consistent system that give $T_c(n, P)$, $T_{fe}(n, P)$, and $\Omega_0^{\perp}(n, P, T)$.

B. FE phase

The observed FE order in STO:Ca has orthorhombic symmetry²⁸. Such states, however, appear as saddle points in the free energy of the the Hamiltonian (3)⁴⁸. Thus, we will assume that the FE ground state has a noncentrosymmetric tetragonal symmetry with an order parameter A along the z saxis. Below T_{fe} , the LO

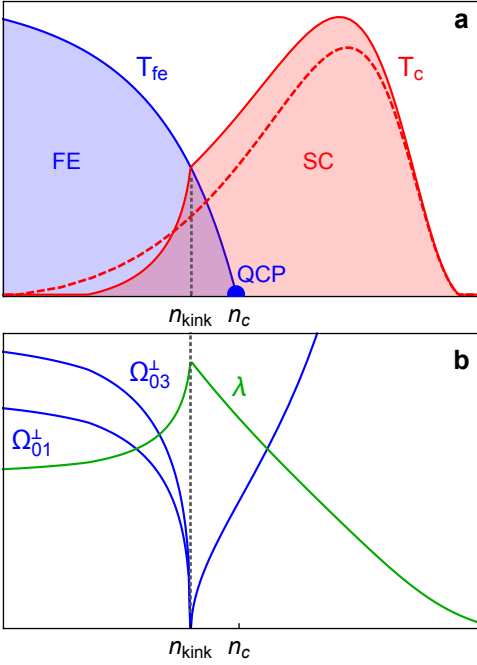


FIG. 1. (a) Schematic phase diagram of our model. Red-solid and red-dashed lines are the SC transition temperatures with and without stress or cation substitution, respectively. (b) Doping dependence of the TO phonon energies $\Omega_{01,3}^\perp$ and SC coupling constant λ along the red-solid phase boundary T_c shown in (a).

frequency becomes anisotropic, while the degenerate PE TO phonon gives rise to two distinct modes,

$$(\Omega_{q1})^2 = (\Omega_{01}^\perp)^2 + B^2 q^2, \quad (9a)$$

$$(\Omega_{q2})^2 = (\Omega_{q1})^2 + [(\Omega_{03}^\perp)^2 - (\Omega_{01}^\perp)^2] \left(\frac{q_\perp}{q}\right)^2, \quad (9b)$$

$$(\Omega_{q3})^2 = (\Omega_{q1})^2 + C^2 + [(\Omega_{03}^\perp)^2 - (\Omega_{01}^\perp)^2] \left(\frac{q_z}{q}\right)^2, \quad (9c)$$

where $q_\perp = \sqrt{q_x^2 + q_y^2}$, Ω_{01}^\perp , and Ω_{03}^\perp are zone-center TO phonons for $\mathbf{q} \perp (001)$ given as follows⁴³,

$$(\Omega_{01}^\perp)^2 = \gamma A^2 + (2\alpha - \gamma)(\psi_1 - \psi_3) + 6e_t \eta_t, \quad (10a)$$

$$(\Omega_{03}^\perp)^2 = 2\alpha A^2, \quad (10b)$$

$$(\Omega_{03}^\perp)^2 = \omega_0^2 + 3\alpha(A^2 + \psi_3) + 2(\alpha + \gamma)\psi_1 - 2e_a \eta_a - 4e_t \eta_t. \quad (10c)$$

$\psi_{1,3} = (2\omega_{1,3})^{-1} \coth(\beta\omega_{1,3}/2)$ are local fluctuations of polarization with $\omega_{1,3} = \sqrt{(\Omega_{01,3}^\perp)^2 + v_0}$, $\eta_a = \langle \eta_1 + \eta_2 + \eta_3 \rangle = (e_a/C_a)(2\psi_1 + A^2 + \psi_3) - P/C_a$, and $\eta_t = \langle \eta_3 - \eta_1 \rangle = (3e_t/2C_t)(A^2 + \psi_3 - \psi_1)$ are volume and deviatoric strains, respectively. Equation (9) shows that the phase volume of critical fluctuations in the FE phase is reduced by the dipolar force.

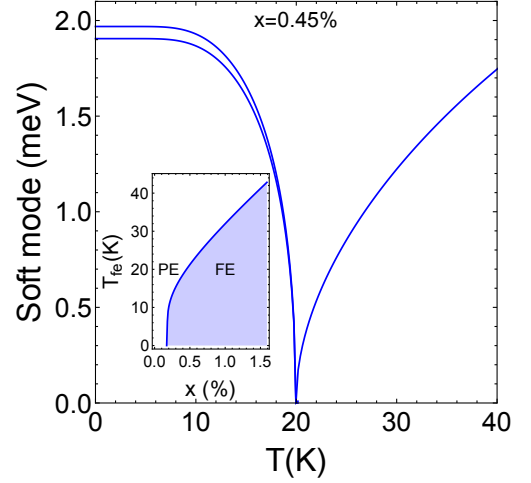


FIG. 2. Calculated TO soft mode frequencies for STO:Ca-0.45% showing the expected split of the high-temperature TO doublet into two modes at the FE transition $T_{fe} \simeq 20$ K. Inset: Calculated phase diagram for STO:Ca- x .

According to Eq. (1), we therefore have,

$$\lambda(n, T_c, P) = \alpha_{e-ph}^2 \sum_{\mathbf{q}} \left(\frac{1}{\Omega_{q1}} + \frac{1}{\Omega_{q2}} + \frac{1}{\Omega_{q3}} \right). \quad (11)$$

Similarly to the PE phase, the critical isotropic TO phonons make the largest contributions to λ .

We assume the same ϵ_F and x dependence of the model parameters as that of the nonpolar phase. Thus, Eqs. (2) and (8)-(11) give the relevant transition temperatures, phonon frequencies, and order parameter in a self-consistent fashion.

III. RESULTS AND DISCUSSION

Figure 1 (a) shows a schematic phase diagram calculated from our model. In the absence of strain or cation substitution, the pairing excitations are PE at all charge densities and we find a dome-shaped T_c similar to the OD models. When long-range polar order is induced by either tuning parameter, we find that it coexists with superconductivity up to a charge density n_c where the FE phase is terminated at the QCP. T_c is enhanced on the PE side whereas it quickly decreases on the FE phase. A kink appears at a charge density n_{kink} , where $T_c = T_{fe}$. Figure 1 (b) shows this is where the TO phonon condenses, which maximizes the coupling constant, as it is shown by the sharp peak in λ .

We now apply our model to n-doped STO:Ca. The model parameters are obtained by fitting to the observed phonon frequencies^{21,25,49}, FE phase diagram,²⁸ and Debye temperature¹² of STO:Ca without doping. The elastic constants were taken from Ref. [50]. As it is usual, we take the continuum limit and replace the summations in Eqs. (7) and (11) by integrals over a

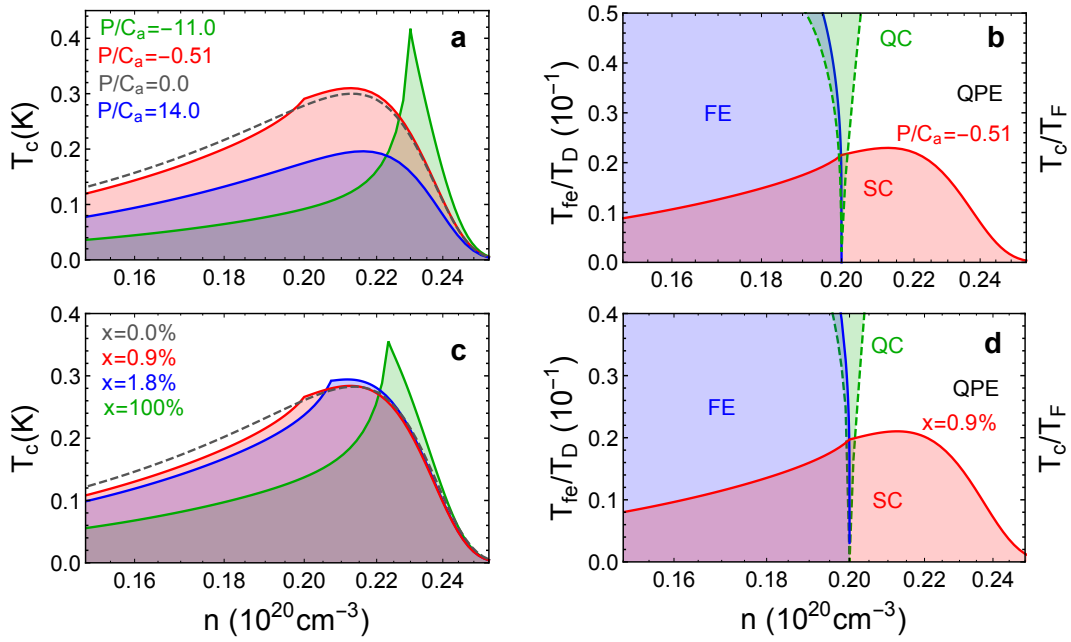


FIG. 3. (a) Calculated T_c for n-doped STO for several negative and positive hydrostatic pressures. (b) Phase diagram for n-doped STO at $P/C_a = -0.51$, showing the overlapping FE phase (blue) and QC region (green). (c) Calculated T_c for n-doped STO:Ca- x . (d) Phase diagram for $x = 0.9\%$.

sphere of wave-vector cutoff radius Λ ⁴⁵. Typical results are shown in Fig. 2 and reproduce well the observed behavior. The parameters b_1, b_2 , and α_{e-ph} are chosen to match the observed QCP in n-doped STO:Ca-0.9% at $n_c \simeq 0.2 \times 10^{20} \text{ cm}^{-3}$ ²¹ and the maximum T_c ($\simeq 0.3 \text{ K}$) for n-doped STO at ambient pressure³. The values are the following: $\omega_0 = 3.9i \text{ meV}$, $\alpha = 7.9 \text{ meV}^3$, $\gamma = 14.8 \text{ meV}^3$, $B = 138.1 \text{ meV \AA}^{-1}$, $C = 7.7 \text{ meV}$, $b_1 = 5.0 \text{ meV}$, $b_2 = 3.4 \times 10^{-16}$, $g = 30.7$, $\Lambda = \pi/a$, $\alpha_{e-ph} = 1.5 \text{ meV}^{1/4}$, $e_a = 4.2 \text{ meV}^2$, $e_t = 0.1 \text{ meV}^2$, $C_a = 7.2 \times 10^4 \text{ meV}$, $C_t = 4.6 \times 10^4 \text{ meV}$.

We first discuss our results for applied hydrostatic pressures. Figure 3 (a) shows the calculated SC domes for several positive and negative pressures. At zero pressure, there is a SC dome shown by the dashed line. Hydrostatic compression pushes the system away from the QCP by hardening the frequency of the TO phonons, therefore decreasing λ as well as T_c . For negative pressures, a QCP is induced within the dome and T_c slightly increases on the PE side while it decreases on the FE side except very near the kink. By increasing negative pressure, the QCP is pushed to higher densities and the dome narrows and sharpens. Figure 3 (b) shows the phase diagram for doped STO under a fixed negative pressure ($P/C_a = -0.51$). T_{fe} and T_c are shown, respectively, in units of T_D and T_F to show that $n_{kink} \lesssim n_c$ and that the kink lies within the QC region $\Omega < T \ll T_D$ ¹⁹. Thus, for STO, we find that the pairing fluctuations near the kink are quantum critical.

We find similar results when the QCP is induced by cation substitution. Figure 3 (c) shows the SC domes

for several Ca concentrations. Inducing a QCP with x also generates a kink at a characteristic charge density n_{kink} . For $n > n_{kink}$, T_c increases, while it decreases for $n < n_{kink}$ except very near the FE transition. Increasing x narrows and sharpens the dome. Figure 3 (d) shows the phase diagram for $x = 0.9\%$. We find again that the kink occurs nearly at the QCP and lies within the QC fan.

We now compare our results to those of previous OD models.^{20,30,31} At the static and qualitative level considered here, our results agree with the essentials of such models in the absence of cation substitution or stress. However, we find that when a FE transition is induced with these tuning parameters, OD models predict a broadening of SC dome and a sharp peak in T_c . This is in stark contrast with our results.

We now compare our results to recent experiments. Our phase diagram is in overall qualitative and fair quantitative agreement with recent experiments in STO:Ca- x ²¹. While an enhancement in T_c is observed near the QCP, the existing data²¹ is too sparse to determine whether there is a kink. Our results are also in qualitative agreement with the observed reduction in T_c with hydrostatic pressure in n-doped STO^{38,39} and the very recent observation of enhanced superconductivity with tensile stress²³. Our calculated dome tends to be narrower than the observed one.²⁻⁵ This is a consequence of our choice of the parametrization given in Eq. (8) for which a theory is clearly needed⁴².

IV. CONCLUSIONS

In summary, by combining a standard model for displacive FEs with a strong-coupling theory of superconductivity, we have studied the effects of a FE quantum phase transition on the SC phase of polar semiconductors and applied it to STO. We have shown that superconductivity is favored by the FE instability from the disordered side, while the increase in dielectric stiffness and dipolar induced anisotropies in the pairing excitations decrease T_c . A kink signature in the dome is generated by the condensation of the phonons when both SC and FE orders set in and when the coupling constant peaks. This generally occurs at charge densities below that of the QCP. When we apply our model to doped STO, we find that the antiadiabatic limit places the kink nearly at its QCP. Our model is in qualitative and fairly quantitative agreement with the recent observation of overlapping FE-like and superconducting instabilities in n-doped STO:Ca- x and the strain tuning of T_c in n-doped STO. At the qualitative and static level considered here, we find that while these results agree with the essentials of previous work invoking OD models to describe the pairing excitations in STO, there are significant differences.

The theoretical framework presented here and its

extensions could provide insight into the intriguing role of spatial inversion symmetry breaking in two-dimensional superconductivity at the interface of STO-based heterostructures,⁵¹ gated KTaO₃⁵², FeSe monolayers on STO⁵³, as well as possible pairing mechanisms with new collective excitations originated by multiferroic QCPs⁵⁴.

Finally, to further explore the possible role of quantum structural transitions on electronic degrees of freedom, we speculate that it may be worthwhile to chemically or electrostatically dope other material candidates near structural QCPs such as the ionic insulators ScF₃⁵⁵ (as recently suggested²³) and the mercuric halide Hg₂I₂⁵⁶.

V. ACKNOWLEDGMENTS

We wish to thank Peter Littlewood and Gilbert Lonzarich for useful discussions. Work at the University of Costa Rica is supported by the Vice-rectory for Research under project no. 816-B7-601, and work at Argonne National Laboratory is supported by the U.S. Department of Energy, Office of Basic Energy Sciences, Materials Science Division under contract no. DE-AC02-06CH11357. G.G.G.V. acknowledges Churchill College, the Department of Materials Science and Metallurgy and the Cavendish Laboratory at the University of Cambridge where part of this work was done.

* Corresponding author: gian.guzman@ucr.ac.cr

¹ J. F. Schooley, W. R. Hosler, and M. L. Cohen, "Superconductivity in semiconducting SrTiO₃," *Phys. Rev. Lett.* **12**, 474 (1964).

² J. F. Schooley, W. R. Hosler, E. Ambler, J. H. Becker, M. L. Cohen, and C. S. Koonce, "Dependence of the superconducting transition temperature on carrier concentration in semiconducting SrTiO₃," *Phys. Rev. Lett.* **14**, 305 (1965).

³ C. S. Koonce, M. L. Cohen, J. F. Schooley, W. R. Hosler, and E. R. Pfeiffer, "Superconducting transition temperatures of semiconducting SrTiO₃," *Phys. Rev.* **163**, 380 (1967).

⁴ G. Binnig, A. Baratoff, H. E. Hoenig, and J. G. Bednorz, "Two-band superconductivity in Nb-doped SrTiO₃," *Phys. Rev. Lett.* **45**, 1352 (1980).

⁵ Hiroshi Suzuki, Hiroshi Bando, Youiti Ootuka, Isao H. Inoue, Tetsuya Yamamoto, Kazuhiko Takahashi, and Yoshikazu Nishihara, "Superconductivity in single-crystalline Sr_{1-x}La_xTiO₃," *J. Phys. Soc. Jpn.* **65**, 1529 (1996).

⁶ D. M. Eagles, "Superconductivity at very low carrier concentrations and indications of a charged bose gas in SrTi_{0.97}Zr_{0.03}O₃," *Solid State Comm.* **60**, 521 (1986).

⁷ D. M. Eagles, R. J. Tainsh, and C. Andrikidis, "Evidence for pairing without superconductivity from resistance between 130 mK and 70 mK in a specimen of ceramic Zr-doped SrTiO₃," *Physica C* **157**, 48 (1989).

⁸ R. J. Tainsh and C. Andrikidis, "Superconducting transitions from states with low normal conductivity in ceramic SrTi_{0.97}Zr_{0.03}O₃," *Solid State Comm.* **60**, 517 (1986).

⁹ D. M. Eagles, "Comment on two papers claiming records for the lowest carrier concentration at which superconductivity has been observed," [arXiv:1604.05660](https://arxiv.org/abs/1604.05660) (2016).

¹⁰ X. Lin, Z. Zhu, B. Fauqué, and K. Behnia, "Fermi surface of the most dilute superconductor," *Phys. Rev. X* **3**, 021002 (2013).

¹¹ J. P. Carbotte, "Properties of boson-exchange superconductors," *Rev. Mod. Phys.* **62**, 1027 (1990).

¹² G. Burns, "Comment on the low temperature specific heat of ferroelectrics, antiferroelectrics, and related materials," *Solid State Comm.* **35**, 811 (1980).

¹³ L. P. Gor'kov, "Phonon mechanism in the most dilute superconductor n-type SrTiO₃," *Proc. Natl. Acad. Sci.* **113**, 4646 (2016).

¹⁴ J. Ruhman and P. A. Lee, "Superconductivity at very low density: the case of strontium titanate," *Phys. Rev. B* **94**, 224515 (2016).

¹⁵ Y. Takada, "Theory of superconductivity in polar semiconductors and its application to n-type semiconducting SrTiO₃," *J. Phys. Soc. Jpn.* **49**, 1267–1275 (1980).

¹⁶ A. Edelman and P. B. Littlewood, "A41.00011 : Polaron-plasmon superconductivity in strontium titanate," *APS March Meeting* (2017).

- ¹⁷ A. G. Swartz, H. Inoue, T. A. Merz, Y. Hikita, S. Raghu, T. P. Devereaux, S. Johnston, and H. Y. Hwang, “Polaronic behavior in a weak-coupling superconductor,” *Proc. Nat. Acad. Sci.* **115**, 1475 (2018).
- ¹⁸ C. Collignon, X. Lin, C. W. Rischau, B. Fauqué, and K. Behnia, “Metallicity and superconductivity in doped strontium titanate,” [arXiv:1804.07067](https://arxiv.org/abs/1804.07067) (2018).
- ¹⁹ S. E. Rowley, L. J. Spalek, R. P. Smith, M. P. M. Dean, M. Itoh, J. F. Scott, G. G. Lonzarich, and S. S. Saxena, “Ferroelectric quantum criticality,” *Nat. Phys.* **10**, 367 (2014).
- ²⁰ J. M. Edge, Y. Kedem, U. Aschauer, N. A. Spaldin, and A. V. Balatsky, “Quantum critical origin of the superconducting dome in SrTiO₃,” *Phys. Rev. Lett.* **115**, 247002 (2015).
- ²¹ C. W. Rischau, X. Lin, C. P. Grams, D. Finck, S. Harms, J. Engelmayer, T. Lorenz, Y. Gallais, B. Fauque, J. Hemberger, and K. Behnia, “A ferroelectric quantum phase transition inside the superconducting dome of Sr_{1-x}Ca_xTiO_{3-δ},” *Nat. Phys.* **13**, 643 (2017).
- ²² A. Stucky, G. W. Scheerer, Z. Ren, D. Jaccard, J.-M. Pomirol, C. Barreateau, E. Giannini, and D. van der Marel, “Isotope effect in superconducting n-doped SrTiO₃,” *Sci. Rep.* **6**, 37582 (2016).
- ²³ C. Herrera, J. Cerbin, K. Dunnett, A. V. Balatsky, and I. Sochnikov, “Strain-engineered interaction of quantum polar and superconducting phases,” [arXiv:1808.03739](https://arxiv.org/abs/1808.03739) (2018).
- ²⁴ K. A. Müller and H. Burkard, “SrTiO₃: An intrinsic quantum paraelectric below 4 K,” *Phys. Rev. B* **19**, 3593 (1979).
- ²⁵ Y. Yamada and G. Shirane, “Neutron scattering and nature of the soft optical phonon in SrTiO₃,” *J. Phys. Soc. Jpn.* **26**, 396 (1969).
- ²⁶ H. Uwe and T. Sakudo, “Stress-induced ferroelectricity and soft phonon modes in SrTiO₃,” *Phys. Rev. B* **13**, 271–286 (1976).
- ²⁷ M. Itoh, R. Wang, Y. Inaguma, T. Yamaguchi, Y.-J. Shan, and T. Nakamura, “Ferroelectricity induced by oxygen isotope exchange in strontium titanate perovskite,” *Phys. Rev. Lett.* **82**, 3540 (1999).
- ²⁸ J. G. Bednorz and K. A. Müller, “Sr_{1-x}Ca_xTiO₃: An xy quantum ferroelectric with transition to randomness,” *Phys. Rev. Lett.* **52**, 2289 (1984).
- ²⁹ P. Chandra, G. G. Lonzarich, S. E. Rowley, and J. F. Scott, “Prospects and applications near ferroelectric quantum phase transitions,” *Rep. Prog. Phys.* **80**, 112502 (2017).
- ³⁰ Y. Kedem, J.-X. Zhu, and A. V. Balatsky, “Unusual superconducting isotope effect in the presence of a quantum criticality,” *Phys. Rev. B* **93**, 184507 (2016).
- ³¹ K. Dunnett, A. Narayan, N. A. Spaldin, and A. V. Balatsky, “Strain and ferroelectric soft-mode induced superconductivity in strontium titanate,” *Phys. Rev. B* **97**, 144506 (2018).
- ³² M. E. Lines and A. M. Glass, *Principles and Applications of Ferroelectrics and Related Materials* (Oxford University Press, 2001).
- ³³ K. Inoue, “Study of structural phase transitions by the hyper-Raman scattering,” *Ferroelectrics* **52**, 253–262 (1983).
- ³⁴ R. Blinc, B. Zalar, V. V. Laguta, and M. Itoh, “Order-disorder component in the phase transition mechanism of ¹⁸O Enriched strontium titanate,” *Phys. Rev. Lett.* **94**, 147601 (2005).
- ³⁵ M. Takesada, M. Itoh, and T. Yagi, “Perfect softening of the ferroelectric mode in the isotope-exchanged strontium titanate of SrTi¹⁸O₃ studied by light scattering,” *Phys. Rev. Lett.* **96**, 227602 (2006); H. Taniguchi, M. Itoh, and T. Yagi, “Ideal soft mode-type quantum phase transition and phase coexistence at quantum critical point in ¹⁸O-Exchanged SrTiO₃,” *Phys. Rev. Lett.* **99**, 017602 (2007); T. Yagi, M. Takesada, M. Taniguchi, and M. Itoh, “Soft-mode dynamics in the ferroelectric phase transition of quantum paraelectric SrTiO₃,” *Ferroelectrics* **379**, 168 (2009).
- ³⁶ K. Rabe, Ch. H. Ahn, and J.-M. Triscone, eds., *Physics of Ferroelectrics: A Modern Perspective* (Springer-Verlag, Berlin, 2007).
- ³⁷ M. Gabay and J.-M. Triscone, “Ferroelectricity woos pairing,” *Nat. Phys.* **13**, 624 (2017); Z. Wang, S. McKeown Walker, A. Tamai, Y. Wang, Z. Ristic, F. Y. Bruno, A. de la Torre, S. Riccò, N. C. Plumb, M. Shi, P. Hlawenka, J. Sánchez-Barriga, A. Varykhalov, T. K. Kim, M. Hoesch, P. D. C. King, W. Meevasana, U. Diebold, J. Mesot, B. Moritz, T. P. Devereaux, M. Radovic, and F. Baumberger, “Tailoring the nature and strength of electron-phonon interactions in the SrTiO₃ (001) 2D electron liquid,” *Nat. Mat.* **15**, 835 (2016); D. van der Marel, J. L. M. van Mechelen, and I. I. Mazin, “Common Fermi-liquid origin of T^2 resistivity and superconductivity in n -type SrTiO₃,” *Phys. Rev. B* **84**, 205111 (2011); J. T. Devreese, S. N. Klimin, J. L. M. van Mechelen, and D. van der Marel, “Many-body large polaron optical conductivity in SrTi_{1-x}Nb_xO₃,” *Phys. Rev. B* **81**, 125119 (2010); W. Meevasana, X. J. Zhou, B. Moritz, C.-C. Chen, R. H. He, S.-I. Fujimori, D. H. Lu, S.-K. Mo, R. G. Moore, F. Baumberger, T. P. Devereaux, D. van der Marel, N. Nagaosa, J. Zaanen, and Z.-X. Shen, “Strong energy-momentum dispersion of phonon-dressed carriers in the lightly doped band insulator SrTiO₃,” *New J. Phys.* **12**, 023004 (2010); J. L. M. van Mechelen, D. van der Marel, C. Grimaldi, A. B. Kuzmenko, N. P. Armitage, N. Reyren, H. Hagemann, and I. I. Mazin, “Electron-phonon interaction and charge carrier mass enhancement in SrTiO₃,” *Phys. Rev. Lett.* **100**, 226403 (2008).
- ³⁸ S. E. Rowley, C. Enderlein, J. Ferreira de Oliveira, D. A. Tompsett, E. Baggio Saitovitch, S. S. Saxena, and G. G. Lonzarich, “Superconductivity in the vicinity of a ferroelectric quantum phase transition,” [arXiv:1801.08121](https://arxiv.org/abs/1801.08121) (2018).
- ³⁹ E. R. Pfeiffer and J. F. Schooley, “Effect of stress on the superconducting transition temperature of SrTiO₃,” *J. Low Temp. Phys.* **2**, 333 (1970).
- ⁴⁰ W. L. McMillan, “Transition temperature of strongly-coupled superconductors,” *Phys. Rev.* **167**, 331 (1968).
- ⁴¹ F. Giustino, “Electron-phonon interactions from first principles,” *Rev. Mod. Phys.* **89**, 015003 (2017).
- ⁴² P. Wölfle and A. V. Balatsky, “Superconductivity at low density near a ferroelectric quantum critical point: Doped SrTiO₃,” *Phys. Rev. B* **98**, 104505 (2018).
- ⁴³ E. Pytte, “Theory of perovskite ferroelectrics,” *Phys. Rev. B* **5**, 3758 (1972).
- ⁴⁴ A. Aharony and M. E. Fisher, “Critical behavior of magnets with dipolar interactions. I. Renormalization group near four dimensions,” *Phys. Rev. B* **8**, 3323 (1973).

- ⁴⁵ J. R. Arce-Gamboa and G. G. Guzmán-Verri, “Random electric field instabilities of relaxor ferroelectrics,” [npj Quantum Materials](#) **2**, 28 (2017).
- ⁴⁶ B. A. Strukov and A. P. Levanyuk, *Ferroelectric Phenomena in Crystals: Physical Foundations* (Springer, Berlin, 1998).
- ⁴⁷ W. Zhong and D. Vanderbilt, “Effect of quantum fluctuations on structural phase transitions in SrTiO₃ and BaTiO₃,” [Phys. Rev. B](#) **53**, 5047 (1996).
- ⁴⁸ R. A. Cowley, “Structural phase transitions I. Landau theory,” [Adv. Phys.](#) **29**, 1 (1980).
- ⁴⁹ G. A. Samara, “The Grüneisen parameter of the soft ferroelectric mode in the cubic perovskites,” [Ferroelectrics](#) **2**, 177 (1971).
- ⁵⁰ M. Carpenter, “Elastic anomalies accompanying phase transitions in (Ca,Sr)TiO₃ perovskites: Part I. Landau theory and a calibration for SrTiO₃,” [Am. Mineral.](#) **92**, 309 (2007).
- ⁵¹ Y.-Y. Pai, A. Tylan-Tyler, P. Irwin, and J. Levy, “Physics of SrTiO₃-based heterostructures and nanostructures: a review,” [Rep. Prog. Phys.](#) **81**, 036503 (2018); S. Gariglio, M. Gabay, and J.-M. Triscone, “Research update: conductivity and beyond at the LaAlO₃/SrTiO₃ interface,” [APL Materials](#) **4**, 060701 (2016).
- ⁵² K. Ueno, S. Nakamura, H. Shimotani, H. T. Yuan, N. Kimura, T. Nojima, H. Aoki, Y. Iwasa, and M. Kawasaki, “Discovery of superconductivity in KTaO₃ by electrostatic carrier doping,” [Nat. Nanotech.](#) **6**, 408 (2011).
- ⁵³ J. J. Lee, F. T. Schmitt, R. G. Moore, S. Johnston, Y.-T. Cui, W. Li, M. Yi, Z. K. Liu, M. Hashimoto, Y. Zhang, D. H. Lu, T. P. Devereaux, D.-H. Lee, and Z.-X. Shen, “Interfacial mode coupling as the origin of the enhancement of T_c in FeSe films on SrTiO₃,” [Nature](#) **515**, 245 (2014).
- ⁵⁴ C. Morice, P. Chandra, S. E. Rowley, G. Lonzarich, and S. S. Saxena, “Hidden fluctuations close to a quantum bicritical point,” [Phys. Rev. B](#) **96**, 245104 (2017); A. Narayan, A. V. Balatsky, and N. A. Spaldin, “Multiferroic quantum criticality,” [arXiv:1711.07989](#) (2017); K. Dunnett, J. X. Zhu, N. A. Spaldin, V. Juricic, and A. V. Balatsky, “Dynamic multiferroicity of a ferroelectric quantum critical point,” [arXiv:1808.05509](#) (2018).
- ⁵⁵ S. U. Handunkanda, E. B. Curry, V. Voronov, A. H. Said, G. G. Guzmán-Verri, R. T. Brierley, P. B. Littlewood, and J. N. Hancock, “Large isotropic negative thermal expansion above a structural quantum phase transition,” [Phys. Rev. B](#) **92**, 134101 (2015).
- ⁵⁶ C. A. Occhialini, S. U. Handunkanda, A. Said, S. Trivedi, G. G. Guzmán-Verri, and J. N. Hancock, “Negative thermal expansion near two structural quantum phase transitions,” [Phys. Rev. Materials](#) **1**, 070603 (2017).